PB90-245317

Prediction of Transient Behavior during Batch Incineration of Liquid Wastes in Rotary Kilns

(U.S.) Environmental Protection Agency, Research Triangle Park, NC

1990

U.S. Department of Commerce
National Technical Information Service
NTIS

AEERL-P-625

TECHNICAL REPORT DATA
(Please read Instructions on the reverse before comple

1. REPORT NO. EPA/600/J-90/056	2.
3 PB90-245317	
4. TITLE AND SUBTITLE Prediction of Transient Behavior During Batch Incineration of Liquid Wastes in Rotary Kilns	5. REPORT DATE
	6. PERFORMING ORGANIZATION CODE
7. AUTHOR(S) J. O. L. Wendt (Univ. of Arizona), and W.P. Linak and P. M. Lemieux (EPA/AEERL)	8. PERFORMING ORGANIZATION REPORT NO.
9. PERFORMING ORGANIZATION NAME AND ADDRESS The University of Arizona Department of Chemical Engineering Tucson, Arizona 85718	10. PROGRAM ELEMENT NO.
	11. CONTRACT/GRANT NO. EPA Purchase Order 9D4636
12. SPONSORING AGENCY NAME AND ADDRESS EPA, Office of Research and Development Air and Energy Engineering Research Laboratory Research Triangle Park, NC 27711	13. TYPE OF REPORT AND PERIOD COVERED Journal article; 10/88 - 12/89
	14. SPONSORING AGENCY CODE EPA/600/13

15. SUPPLEMENTARY NOTES AEERL project officer is William P. Linak, Mail Drop 65, 919/541-5792. Hazardous Waste and Hazardous Materials, Vol. 7, No. 1, pp. 41-54, Winter 1990.

16. ABSTRACT The paper discusses a theoretical model which was designed to: (1) provide insight into why, for liquid wastes, "puffs" are very easily generated, and why their magnitudes and intensities increase with increasing kiln temperature and speed of rotation; and (2) predict how the generation of puffs in general is controlled by waste properties, sorbent properties, and kiln operating parameters. When containerized liquid wastes, bound on sorbents, are introduced into a rotary kiln in a batch mode, transient phenomena involving vaporization of the waste, and mass and heat transfer into the sorbent can allow a rapid release of water vapor into the kiln environment, a displacement of excess oxygen from the primary flame, and formation of a puff. This transient puff then travels to the afterburner and, if it is too large, can result in a failure mode of the incinerator system. Previous experimental work has been performed by EPA on a specially designed rotary kiln incinerator simulator.

17. KEY WORDS AND DOCUMENT ANALYSIS

a. DESCRIPTORS		b. IDENTIFIERS/OPEN ENDED TERMS	c. COSATI Field/Group	
Pollution	Transient Response	Pollution Control	13B	14G
Combustion	Mathematical Models	Stationary Sources	21B	12A
Incinerators	Predictions	Liquid Wastes		
Kilns		Rotary Kilns	13A	
Liquids		Puffs	07D	
Waste Disposal				

18. DISTRIBUTION STATEMENT Release to Public	19. SECURITY CLASS *(This Report)* Unclassified	21. NO. OF PAGES 15
	20. SECURITY CLASS *(This page)* Unclassified	22. PRICE A03

EPA Form 2220-1 (9-73)

REPRODUCED BY
U.S. DEPARTMENT OF COMMERCE
NATIONAL TECHNICAL
INFORMATION SERVICE
SPRINGFIELD, VA 22161

PB90-245317

EPA/600/J-90/056

HAZARDOUS WASTE & HAZARDOUS MATERIALS
Volume 7, Number 1, 1990
Mary Ann Liebert, Inc., Publishers

NTIS is authorized to reproduce and sell this report. Permission for further reproduction must be obtained from the copyright owner.

Prediction of Transient Behavior During Batch Incineration of Liquid Wastes in Rotary Kilns

J. O. L. WENDT

Department of Chemical Enginering
University of Arizona
Tucson, AZ 85718

W. P. LINAK and P. M. LEMIEUX

Air and Energy Engineering Research Laboratory
U.S. Environmental Protection Agency
Research Triangle Park, NC 27711

ABSTRACT

When containerized liquid wastes, bound on sorbents, are introduced into a rotary kiln in a batch mode, transient phenomena involving vaporization of the waste, and mass and heat transfer into the sorbent can allow a rapid release of waste vapor into the kiln environment, a displacement of excess oxygen from the primary flame, and formation of a "puff." This transient puff then travels to the afterburner and, if it is too large, can result in a failure mode of the incinerator system. Previous experimental work by the U.S. Environmental Protection Agency on a specially designed Rotary Kiln Incinerator Simulator has shown that, for liquid wastes, puffs are very easily generated, and that their magnitudes and intensities increase with increasing kiln temperature and increasing kiln rotation speed. This paper presents a theoretical model which was designed both to provide insight into why this is so, and to predict how the generation of puffs in general is controlled by waste properties, sorbent properties, and kiln operating parameters.

INTRODUCTION

The objectives of this research were to develop insight into mechanisms which govern the generation of transient puffs resulting from the batch introduction into the firebox of a rotary kiln incinerator of containerized liquid wastes bound on sorbents. Parametric experimental studies, reported by Linak et al. (1)(2), have shown that puffs are very easily generated even at high excess air values of the primary flame, and that, contrary to standard incineration practice, both the puff intensity and the puff magnitude increased with increasing kiln temperature.

These experimental studies were completed on a laboratory rotary kiln incinerator simulator, shown on Figure 1. Cardboard containers of liquid wastes, bound on sorbents, were introduced into the kiln firebox cavity through the sliding gate using the charging basket/ram assembly shown. Products of incomplete combustion in the exhaust were measured as a function of time. Data were analyzed empirically using statistical methods involving response surfaces and quadratic models which contained all the statistically significant linear and quadratic interactions.

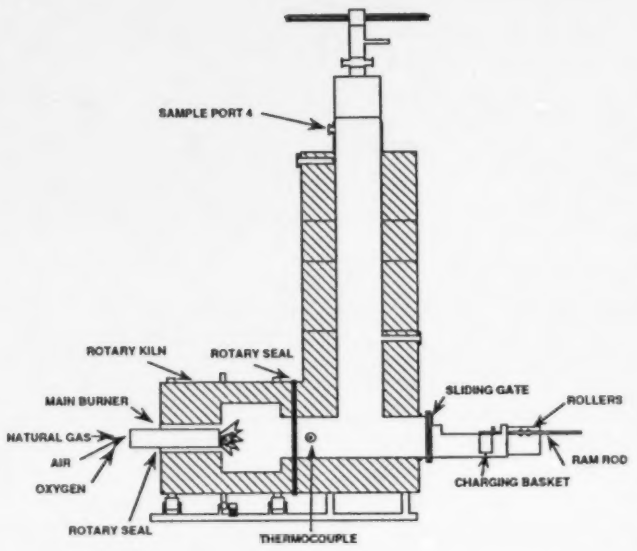

Figure 1. Rotary Kiln Incinerator Simulator.

The purpose of the research reported in this paper was to put our understanding of the observed phenomena onto a mechanistic footing and, by so doing, to gain a more fundamental insight into how and why certain kiln, waste, and sorbent parameters have the effects that they do. A mechanistic model, grounded on known principles of heat and mass transfer, can support the experimental studies by showing the general applicability of the results obtained. In addition, a mechanistic model is amenable to extrapolation to conditions outside the experimental test matrix, while a purely empirical model is not. Therefore, a successful mechanistic model, which correctly describes how kiln parameters and waste properties influence transient puff behavior, not only can be used to correlate existing data with properties of wastes that have been examined, but also can rank a much wider range of liquid wastes according to the propensity of each to cause a transient puff that may overload the system and precipitate a failure mode of operation.

Only containerized liquid wastes bound on sorbents are considered in this work. We make no attempt to describe all the events likely to occur in the rotary kiln combustion chamber after the introduction of the container. Rather our attention is focused solely on the sorbent originally in the container, and on the rate of evolution of gaseous waste out of the sorbent into the hot kiln environment. The model was designed to test the hypothesis that transient puffs are controlled by the rapid evolution of waste gases from the containerized sorbent, rather than by the mixing of the waste vapor with the flue gases from the primary flame. This is certainly not be true as far as the composition of the puff is concerned, since data (1)(2) conclusively show the presence of partially oxygenated products of incomplete combustion (PICs) in the puff. However, all the data show that puff magnitude and puff intensity increase, as contacting is enhanced between the waste-sorbent aggregate and the oxygen containing primary flame flue gas. This suggests that heat transfer to the sorbent and/or mass transfer from the sorbent (both surface area dependent phenomena) control the phenomena being investigated, rather than events occurring in the gas phase where better mixing would <u>decrease</u> puff intensity. We recognize that the situation is further complicated by the fact that measurements of both puff intensity and puff magnitude depend on the nature of the species actually measured and deemed to represent those quantities. Therefore, there may be a second order effect of gas phase mixing, but this is not considered here.

Furthermore, we do not consider the mechanism of rupture or destruction of the actual container holding the sorbent/waste mixture. The model focusses only

on events occurring after the walls of the container cease to be a factor in restraining the evolution of mass. Therefore, the model is more applicable to combustible cardboard containers than to steel drums, for which very different aggregate surface exposure models might apply. The remainder of the paper is divided into the following parts: (1) a review of existing experimental data, since those are to be simulated by the model; (2) a presentation of the mathematical model, the physical rationale behind its derivation, and the equations to be solved; (3) a description of the numerical techniques used to solve the equations; (4) a presentation of model results and comparisons with data; and (5) discussions of conclusions from this study, practical implications to be drawn, and suggestions for future work.

EXISTING DATA

The experimental results which motivated the theoretical work presented here were obtained from the rotary kiln incinerator simulator shown on Figure 1. This 73 kW (250,000 Btu/hr) prototype thermal destruction unit was designed to include the salient features of practical kilns, but still be sufficiently versatile to allow parametric experimentation by varying selected parameters one at a time or by controlling a set of parameters independently. This laboratory combustor has been described in detail elsewhere (2), and only those aspects crucial to an understanding of the model are presented here. We are concerned not with the afterburner section (which follows the kiln) but only with the kiln itself and the transition section. Internal radial dimensions vary from 0.762m (30 in.) in the kiln recess to 0.457m (18 in.) in the transition and tower sections. Linak et al.(2) compare the design and operation of the simulator to full scale units and conclude that this is a valid prototype experimental configuration and that results from this simulator do relate to full scale units.

When the closed cardboard container holding liquid waste bound on sorbent (ground corn cob material, in this case) is rammed into the kiln furnace and falls into the recessed cavity it takes a few seconds for the cardboard to disintegrate. Thereupon, the contents are exposed to the hot kiln environment, and waste is released from the sorbent aggregate. Time resolved measurements of the transient puff produced may consist of total hydrocarbons (THCs) reported as parts per million methane.

Figure 2 depicts experimental puff traces for four replicate tests with fuel oil as a surrogate waste. Clearly there are significant differences between

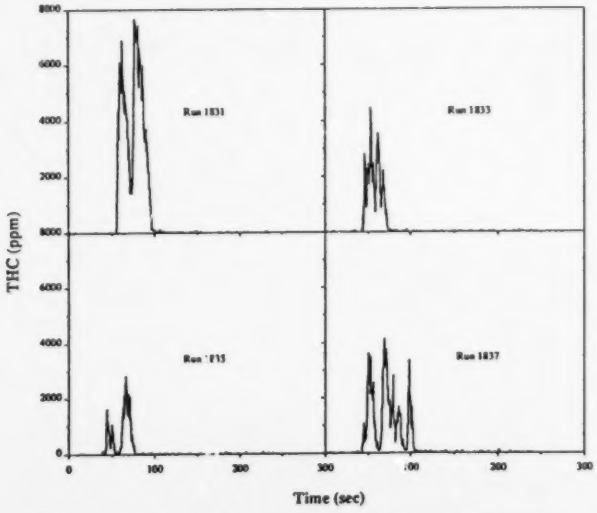

Figure 2. Experimental Puff Intensity Traces. Surrogate waste is No. 5 Fuel Oil.

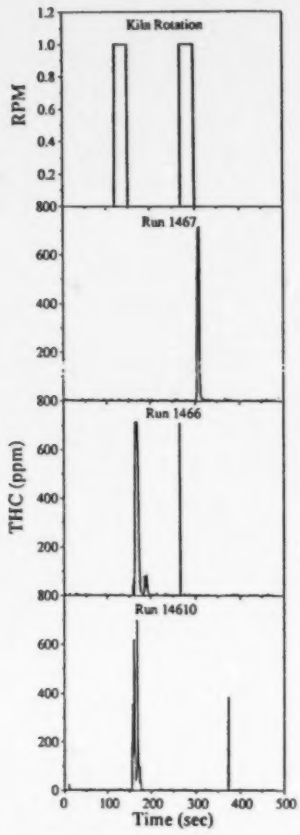

Figure 3. Results from Special Experiment.

replicate test results, indicating the existence of random phenomena. There are, however, some important similarities. First, note how the duration of a puff can last up to 100 seconds, even though the boiling point of the waste is greatly exceeded in the kiln. This demonstrates the importance of heat and mass transfer rate limitations to the evolution of waste out of the sorbent aggregate. Note also that the puff traces are characterized by a coarse structure of two or more sharp peaks on which there is superimposed a fine structure of smaller fluctuations. We might attribute the coarse structure to discrete events during which new surface of the sorbent aggregate is being exposed to the kiln environment, while the fine structure results from turbulent mixing in the gas phase.

If the above hypothesis is valid, the sharp transient peaks comprising the coarse structure should be correlated with the rotation of the kiln. We have observed that in our simulator, the aggregate initially adheres to the kiln walls and thus rotates for about a quarter of a revolution until it falls and breaks up to expose new surface. Figure 3 shows results of a special experiment that was performed to illustrate this point. The kiln was allowed to rotate for less than half a revolution and then stopped, and this procedure was completed twice for each run, as shown on the top panel of the figure. The puff traces shown below for three separate runs support the hypothesis that new surface exposure occurs in a discrete but not always reproducible fashion, and that when this occurs it does so at approximately one quarter of a revolution. It is possible, however, for a new surface exposure event not to occur (see second panel on Figure 3), in which case the aggregate merely slides back to its original position, rather than falling back and fragmenting. The fourth panel on Figure 3 suggests also that

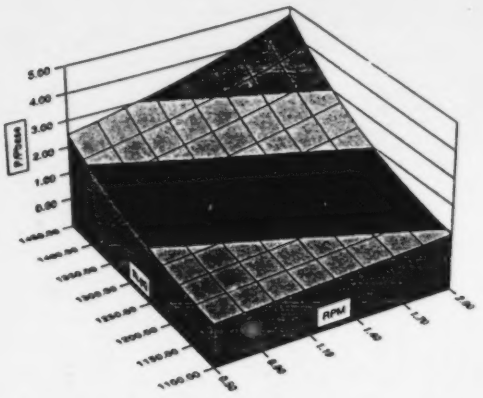

Figure 4. Measured Puff Magnitude as Function of T_k and RPM.

surface renewal events do not always occur at exactly the same angle of rotation of the kiln.

Figure 4 depicts the dependence of relative puff magnitude on kiln RPM and kiln temperature. These results are for toluene as a surrogate waste. Puff magnitudes are measured by the weight of particulate matter collected on a filter, and are normalized by the value at the "base case" condition of T_k=1250 K and RPM=0.5 rpm. Clearly puff magnitude increases with kiln RPM and kiln temperature, and a useful model should be able to simulate these effects.

MODEL

The shape and duration of the hydrocarbon traces shown on Figure 2 strongly suggest that transport phenomena, and not only vapor-pressure driving forces, modulate the evolution of waste material into the bulk gas phase. The strong effect of kiln rotation speed suggests that the rate of mass evolution depends on the rate at which new surface is exposed to the hot kiln environment and that this facet should be included in the model. Our approach was to formulate an idealized prototype model which, hopefully, correctly describes the salient features present in the practical case, without omitting any physical phenomenon of first order importance. The tumbling motion of the sorbent/waste is extremely complex and it is not worthwhile to attempt to model that in scrupulous detail.

The model developed consists of two parts (Figure 5): the first comprises the prototype problem of transient simultaneous heat and mass transfer in a sorbent aggregate layer, coupled with local vaporization rates depending on local vapor pressure and local composition; the second comprises the surface exposure model which assumes that surface renewal occurs every quarter of a revolution (see Figure 3). The amount of new surface area created at each event is not known and is, in fact, a random quantity. We assume that, at each surface renewal event, the entire aggregate, and not each fragment, breaks up into four new pieces. This means that the surface available for mass transfer increases at the first event but, although it is renewed at every subsequent event, it no longer increases in value. In a previous model (3) the surface area increased geometrically with fragmentation and the time between events depended on aggregate size. The current approach, however, does not attempt to describe the motion of the bed in detail (4).

Consider time dependent, simultaneous heat and mass transfer in a sorbent aggregate, as shown on Figure 5 (upper portion). The sorbent aggregate is composed of individual sorbent particles, each of which locally releases vapor into the interstitial gas volume at a rate determined by the local particle drying rate. The gas evolved diffuses through the voids to the surface, and is released to the kiln environment. The local particle drying rate depends on the

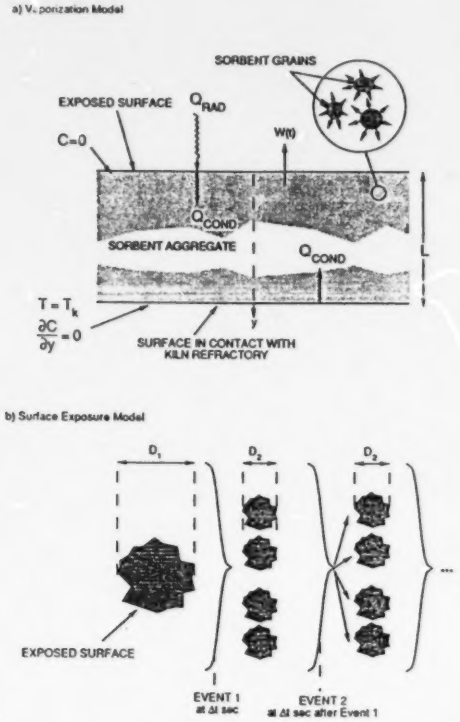

Figure 5. Schematic of Model.

local value of the waste vapor pressure, and thus on the local temperature, as determined from the transfer of heat.

In the equations that follow, symbols not listed in the nomenclature have their usual meaning in the context within which they are presented.

Equations to be solved are:

Energy:

$$\frac{\partial T}{\partial t} = \frac{k}{(1-\epsilon)\, C_p\, \rho} \frac{\partial^2 T}{\partial y^2} - \frac{\Delta H_v}{C_p\, \rho} R_v\,(T,\, C,\, C_s) \tag{1}$$

Species in the interstitial gas phase:

$$\frac{\partial C}{\partial t} = D_{eff} \frac{\partial^2 C}{\partial y^2} + (1-\epsilon)\, R_v\,(T,\, C,\, C_s) \tag{2}$$

Species within/on sorbent particles:

$$\frac{\partial C_s}{\partial t} = -R_v\,(T,\, C,\, C_s) \tag{3}$$

The local vaporization rate, $R_v(t,y)$, is of the form:

$$R_v\,(T,\, C,\, C_s) = \frac{12\, D_m}{d_g^2} \left\{ \frac{P^{vap}}{RT} \frac{C_s}{C_{crit}} - C \right\} \tag{4}$$

when C_s is less than C_{crit}; i.e., when the falling rate applicable to drying theory is applicable. For regimes where constant drying rate can be locally applied:

$$R_v\ (T,\ C) = \frac{12\ D_m}{d_g^2}\ (\frac{P^{vap}}{RT} - C) \tag{5}$$

Here it has been assumed that the Sherwood Number for an individual grain is equal to 2 and that the grains are spherical. Clausius Clapyron yields:

$$P^{vap}\ (T) = A \exp\ (-\Delta H_v/RT) \tag{6}$$

and the effective diffusivity is assumed to have the form:

$$D_{eff} = D_m \times \epsilon^2 = \frac{0.0018583\ [T^3\ (\frac{1}{29} + \frac{1}{MW})]^{1/2}}{p\ \sigma_{AB}^2} \times \epsilon^2 \tag{7}$$

The initial conditions are:

$$t = 0, \quad T = T_o, \quad C = C_o, \quad C_s = C_{so}$$

The boundary conditions are:

$$\begin{aligned} y = 0 \quad & -k \frac{\partial T}{\partial y} = \epsilon\sigma\ (T_k^4 - T^4), \quad C = 0 \\ y = L \quad & T = T_k \quad , \quad \frac{\partial C}{\partial y} = 0 \end{aligned} \tag{8}$$

The only completely unknown adjustable parameter is C_{crit}, which defines the onset of the falling drying rate. Because the equations are non linear, and strongly coupled through the steep dependence of vapor pressure on temperature, analytical solution to obtain

$$N_A(t)\ \Big|_{y=0} = -\ D_{eff}\ \frac{\partial C}{\partial y}\ \Big|_{y=0} \tag{9}$$

as a function of time, and thus the total flux of waste leaving the surface, as a function of time, is difficult. Therefore, numerical solution of the above equations was attempted.

Solution of these equations yields the total mass flux of waste leaving the surface as a function of time. This quantity, multiplied by surface area, yields the "Unsatisfied Oxygen Demand" which defines puff intensity, thus:

$$Y_{O_2}^* = Y_{O_2} - \nu \frac{F_w}{F_f}$$

$$\begin{aligned} \text{Unsatisfied Oxygen Demand} &= 0\ , \quad Y_{O_2}^* \geq 0 \\ &= -Y_{O_2}^*\ F_f,\ Y_{O_2}^* < 0 \end{aligned} \tag{10}$$

The time interval between surface exposure events is now given by:

$$\Delta t = 0.25\ (\frac{60}{RPM}) \tag{11}$$

The equations were non-dimensionalized:

$$\theta = \frac{T - T_o}{T_k - T_o}$$

$$\phi = \frac{C}{C_{max}} \qquad (12)$$

$$\xi = \frac{C_s}{C_{so}}$$

and resulting dimensionless equations were solved numerically using a fully implicit algorithm and finite differencing with a variable mesh. This is briefly described below, since it contains some novel attributes.

Distance into the sorbent from the exposed surface was represented by a mesh with unequally spaced grid points. The finest mesh was at each surface, since that is where the steepest gradients were anticipated. For the results reported here, a collapsing factor of 2 (i.e., $DY_{p+1} = 2. \times DY_p$) provided adequate spatial resolution. Discretization in the time domain was with a constant step size, determined by dividing the interval between each pair of fragmentation events by 25. This form of finite differencing led to the following difference equations:

$$\alpha_T \theta_{p-1}^{k+1} + \beta_T \theta_p^{k+1} + \gamma_T \theta_{p+1}^{k+1} = - \frac{a_2}{(T_k - T_o)} R_p^{k+1} - \frac{\theta_p^k}{\Delta t} \qquad (13)$$

where:

$$\alpha_T = \left(\frac{a_1 2}{\Delta y_{p+1} + \Delta y_{p-1}}\right)\left(\frac{1}{\Delta y_{p-1}}\right)$$

$$\beta_T = \left(\frac{a_1 2}{\Delta y_{p+1} + \Delta y_{p-1}}\right)\left(-\frac{1}{\Delta y_{p-1}} - \frac{1}{\Delta y_{p+1}}\right) - \frac{1}{\Delta t} \qquad (14)$$

$$\gamma_T = \left(\frac{a_1 2}{\Delta y_{p+1} + \Delta y_{p-1}}\right)\left(\frac{1}{\Delta y_{p+1}}\right)$$

For dimensionless concentration:

$$\alpha_c \phi_{p-1}^{k+1} + \beta_c \phi_p^{k+1} + \gamma_c \phi_{p+1}^{k+1} = - \frac{b_2}{c_{max}} R_p^{k+1} - \frac{\phi_p^k}{\Delta t} \qquad (15)$$

with α_c, β_c, and γ_c calculated analogously to α_T, β_T, and γ_T.

For sorbent concentration:

$$- \frac{\xi_p^{k+1}}{\Delta t} = \frac{c_2}{C_s^o} R_p^{k+1} - \frac{\xi_p^k}{\Delta t} \qquad (16)$$

In these equations, the coefficients a_1, a_2, b_1, b_2, and c_2 are combinations of parameters appearing in Equations (1) through (3) and occurring naturally during non-dimensionalization.

Stability of the finite difference equations outlined above is improved if the source term on the right hand side can be evaluated at the new k+1 step;

i.e., if the system can be solved fully implicitly. Following Wendt et al. (5), the new values of the right hand side can be estimated by expanding the source term in a Taylor Series about the backward point, thus:

$$R_p^{k+1}(\theta, \phi, \xi) = R_p^k + \left.\frac{\partial R}{\partial \theta}\right|_p^k (\theta_p^{k+1} - \theta_p^k) + \left.\frac{\partial R}{\partial \phi}\right|_p^k (\phi_p^{k+1} - \phi_p^k) + \left.\frac{\partial R}{\partial \xi}\right|_p^k (\xi_p^{k+1} - \xi_p^k) \quad (17)$$

This results in a block tridiagonal matrix, which is also a banded matrix, and which must be inverted to yield the new values of θ, ϕ, and ξ. In this program the inversion was by Gaussian elimination modified to operate only on banded matrices.

At each surface renewal event a new "initial" average aggregate temperature and waste concentration were calculated from the temperature profile in the aggregate and the total amount of waste removed by the end of the previous event. Thus, at the beginning of each event, the "initial" temperature throughout the sorbent increased, and the "initial" amount of waste on the sorbent decreased as the process proceeded. When all of the original waste had been removed the process was considered to be at an end, and only then was combustion of the sorbent aggregate allowed to start. This process is not considered in the model presented here, since it was shown that sorbent combustion without waste absorbed did not lead to puffs.

Numerical integration in the y direction over the unequally space grids was accomplished by the Trapezoidal Rule while that in the time direction (equally spaced grid points) used Simpson's Rule. These integrations were necessary to calculate average temperatures at the end of a fragmentation interval, and total fluxes of waste out of the sorbent aggregate surface over that time interval. For the latter, the following represents the instantaneous flux of waste at time t, given by time mesh point k:

$$N_A^k = - D_{eff} \left[- \frac{(2\Delta y_1 + \Delta y_2)}{\Delta y_1 (\Delta y_1 + \Delta y_2)} C_1^k + \frac{(\Delta y_1 + \Delta y_2)}{\Delta y_1 + \Delta y_2} C_2^k - \frac{\Delta y_1}{\Delta y_2 (\Delta y_1 + \Delta y_2)} C_3^k \right]$$

The only completely unknown parameters in this model are C_{crit} and the number of fragments causing surface renewal at each event. Here, the latter quantity was taken to be four, and the former was chosen to yield reasonable comparisons with data at zero kiln rotation speed, i.e. with no surface renewal. Other parameters result from waste, kiln and sorbent specifications and have been presented elsewhere (3).

MODEL RESULTS

Figure 6 shows predictions of time resolved traces of waste evolution rate, mole fraction O_2 downstream of the puff, and the puff intensity itself, as defined by the O_2 deficit (Equation 10). These predictions (for fuel oil as a surrogate waste) should be compared to the experimental traces on Figure 2. The duration of the puff and its coarse structure are predicted reasonably well. Figure 6 also shows that appreciable quantities of waste do not begin to evolve until the first surface renewal event has occurred. This is in agreement with the data shown on Figure 3. A puff is predicted to occur only when the oxygen has fallen to zero, and this, it should be emphasized, completely neglects any mixing inhomogeneities in the gas phase.

Further insight into the chemical and physical processes that are important can be gained by examining the spatial profiles of temperature, interstitial waste concentration, and waste concentration on sorbent. These are presented on Figures 7,8 9 and 10 for the period between 60sec and 75sec, i.e. during the first puff peak shown on Figure 6. The temperature profile shows that direct contact heating of the aggregate by the kiln surface does cause rapid heating up at the boundary through which waste cannot escape. This portion of the temperature profile has a large influence on the average temperature to be experienced at the next event. The radiation heat flux boundary condition at y=0 leads to a very steep temperature gradient at the free surface, but not much

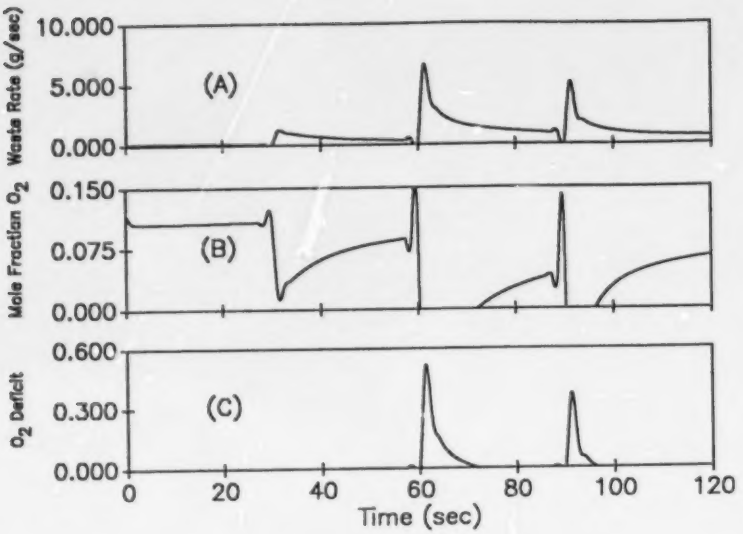

Figure 6. Predicted Puff Trace.

penetration (Figure 8). Interstitial gas-phase waste concentrations (Figure 9) are very high at the surface in contact with the kiln refractory, but do not diffuse sufficiently rapidly to influence the flux at y=0. This quantity appears to be controlled solely by the temperature rise very close to the free surface. Concentrations on the sorbent aggregate (Figure 10) show depletion at the free surface, as expected, and some re-absorption at the far side, due to the wave of high gas-phase waste concentrations travelling from left to right (Figure 9). The model allows for the local evolution rate to be positive or negative, but we are not certain that this is physically reasonable. In any case, this re-absorption process, if it exists, does not influence the waste flux at y=0, which is the quantity of interest.

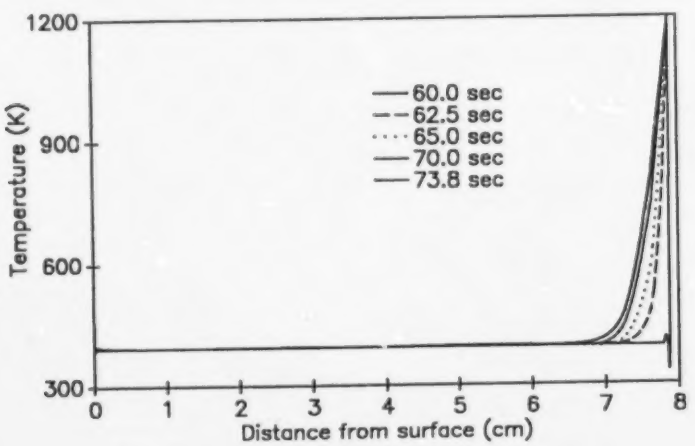

Figure 7. Temperature Profile in Aggregate.

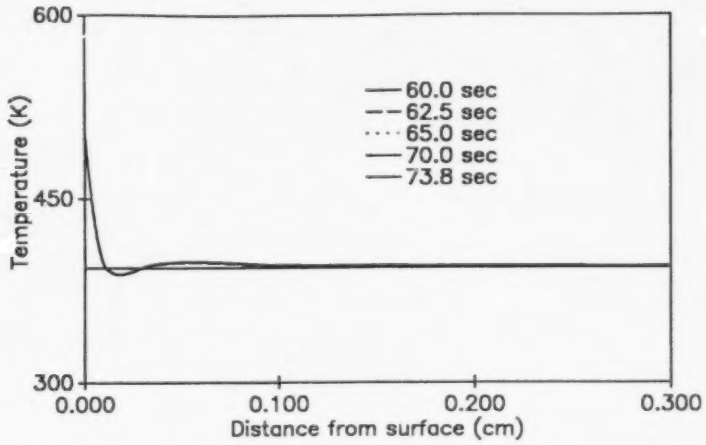

Figure 8. Detail from Figure 7 Showing Heat Flux Boundary Condition.

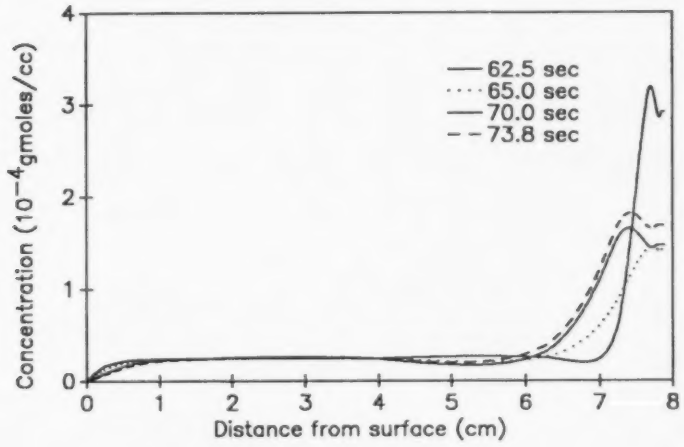

Figure 9. Interstitial Waste Concentration Profile

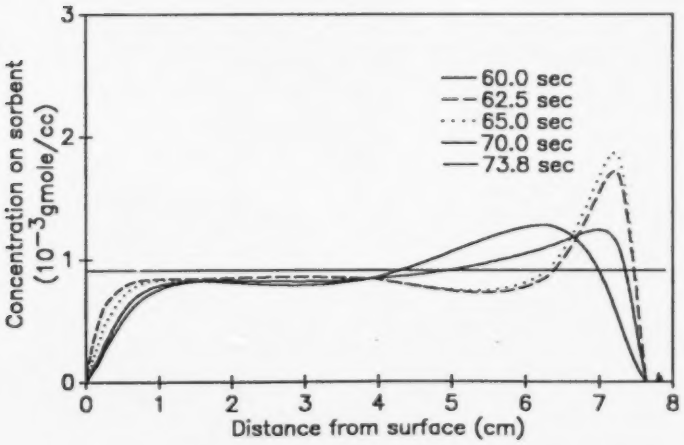

Figure 10. Waste Concentration on Sorbent Profile

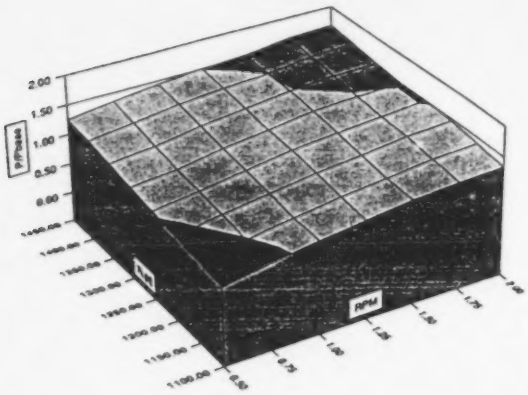

Figure 11. Predicted Puff Magnitude as Function of T_k and RPM.

Figure 11 shows predicted results of the effects of kiln rotation speed and kiln temperature on puff magnitude, the integral under the puff intensity trace. Results are for toluene and have been normalized relative to a base case as shown. This figure should be compared to Figure 4 which shows data for the same waste and sorbent. The effects of both kiln temperature and kiln rotation speed are well predicted. Quantitative discrepancies might well be removed by further adjustment of one of the two arbitrary parameters in the model, namely the number of fragments formed at each event. However, taken as a whole, the results of this model are encouraging, and suggest that it provides a useful basis on which to build future models.

CONCLUSIONS

A model describing the generation of puffs during the batch incineration of liquid wastes bound on sorbents is described. Agreement between predictions and data is good, especially in view of the complexities and randomness of rotary kiln phenomena.

The unsteady vaporization/surface renewal model not only supports existing experimental data but also explains why the effects of kiln temperature and kiln rotation speed occurred. The mechanistic understanding provided thereby suggests that puffs can occur very easily in practice and in the field, and they can last a relatively long time. The intensity and magnitude of a puff depends strongly on kiln, waste, and sorbent parameters. Container dimensions are important only in so far as they affect the bulk porosity of the sorbent.

This model may be used to rank wastes and sorbents with respect to producing puffs. Waste boiling point, and therefore waste latent heat, is as important as the more obvious stoichiometric oxygen requirement of the waste. Kiln operation that allows high partial pressures of oxygen simultaneously with low kiln temperatures can alleviate puff problems. Low kiln rotation speed is always desirable.

Future work may be usefully employed in fine tuning the surface renewal model, with a view to obtaining better quantitative agreement between theory and experiment. Difficulties in accurately measuring puff properties may obfuscate this objective. Ultimately, mixing in the gas phase in the kiln environment must also be considered.

Throughout this paper we have focussed only on events occurring in the kiln itself, prior to the afterburner. Therefore we have addressed the problem of predicting transient phenomena which must be handled by the afterburner in order to safely operate a rotary kiln system. Future work is also needed to address the problem of transient inputs into an afterburner system.

ACKNOWLEDGEMENTS

Portions of this work were conducted under EPA Purchase Order 9D4636NATA with J.O.L.Wendt.

DISCLAIMER

The research presented here has been reviewed by the Air and Energy Engineering Research Laboratory of the U.S. Environmental Protection Agency and approved for publication. The contents of this article should not be construed to represent Agency policy nor does mention of any procedures, trade names or commercial products constitute endorsement or recommendation for use.

NOMENCLATURE

C	Concentration in interstitial gas phase
C_s	Concentration on sorbent
C_p	Specific heat of sorbent (cal/gK)
d_g	Sorbent grain size (cm)
D_{eff}	Effective diffusivity
D_m	Molecular diffusivity (cm^2/sec)
F_f	Molar flow of flue gas (gmoles/s)
F_w	Mass flow of waste out of surface (g/sec)
k	Thermal conductivity of sorbent (cal/scmK)
N_A	Flux of waste at surface (moles/cm^2-sec)
P	Pressure (atm)
P^{vap}	Vapor pressure of waste (atm.)
R_v	Vaporization rate (gmoles/cc-sec)
R	Gas constant
T	Temperature (K)
T_k	Kiln temperature (K)
t	Time (sec)
$Y^*_{O_2}$	O_2 Mole fraction after consuming evolved waste
Y_{O_2}	O_2 Mole fraction in primary flame flue gas

Greek Symbols

ϵ	Bulk porosity
θ	Dimensionless temperature

ϕ Dimensionless concentration (gas)

ξ Dimensionless concentration on sorbent

ν Stoichiometric requirement of waste (gmoles O_2 required/g waste)

REFERENCES

1. Linak, W.P., McSorley, J.A., Wendt, J.O.L. and Dunn, J.E., J. Air Poll. Cont. Assoc., 37:934-942 (1987a).

2. Linak, W.P., Kilgroe, J.D., McSorley, J.A., Wendt, J.O.L. and Dunn, J.E., J. Air Poll. Cont. Assoc., 37:54-65 (1987b).

3. Wendt, J.O.L., and Linak, W.P., Combustion Sci. and Tech., 61, 169 (1988).

4. Zablotny, W.W., J. Internl. Chem. Eng., 5, (2), 360 (1965).

5. Wendt, J.O.L., Martinez, C.M., Lilley, D.M. and Corley, T.L., Chem. Eng. Sci., 34:527 (1979).